

# Fatigue behavior of fiber-reinforced concrete in compression

Paulo B. Cachim <sup>a,\*</sup>, Joaquim A. Figueiras <sup>b</sup>, Paulo A.A. Pereira <sup>c</sup>

<sup>a</sup> *SAECivil, Civil Engineering Department, University of Aveiro, 3810 Aveiro, Portugal*

<sup>b</sup> *Civil Engineering Department, University of Porto, 4050-123 Porto Codex, Portugal*

<sup>c</sup> *Civil Engineering Department, University of Minho, 4800 Guimaraes, Portugal*

Received 6 October 2000; accepted 2 April 2001

---

## Abstract

An experimental program has been carried out to evaluate the performance of plain concrete and fiber-reinforced concrete under compressive fatigue loading. Two types of hooked-end steel fibers (30 mm length and 60 mm length) have been tested and their performance compared. The displacements and the acting load were measured during the tests so that several material parameters could be identified and assessed. Wöhler diagrams were determined, cyclic creep curves were plotted and the evolution of the secant stiffness was also appraised for the tested materials. The correlation between the secondary creep rate and the fatigue life was investigated. The monotonic stress–strain envelope was compared with fatigue deformations at failure and a good agreement was found between them. © 2002 Elsevier Science Ltd. All rights reserved.

**Keywords:** Fatigue tests; Concrete fatigue; Concrete; Fiber-reinforced concrete; Steel fibers

---

## 1. Introduction

The search for construction materials with enhanced properties such as strength, ductility, toughness and durability has lead to an increasing interest in materials like fiber concrete and high-performance concrete. The limited knowledge about the long-term behavior or the effects of repeated loading on the properties of these materials has caused a growing interest on the fatigue performance of concrete [4,5,7,8,11,13,15]. Additionally, reliable data are needed for the calibration of accurate models capable of predicting the fatigue behavior of structural concrete.

The most important improvement attained by the addition of fibers to concrete is the increase in toughness and ductility [18]. Nevertheless, it is also possible to improve other properties such as the strength and stiffness [13]. In practical applications, however, steel fibers are added in percentages of about 0.5% in volume (40 kg/m<sup>3</sup>) for which it is unlikely to obtain higher strengths. Hooked-end steel fibers seemed to be the most effective steel fibers in terms of toughness improvement [13].

## 2. Materials, equipment and test procedure

The experimental test program has been carried out at the Laboratory of Structures of the Faculty of Engineering of the University of Porto in Portugal. The concrete composition is summarized in Table 1. Two types of hooked-end steel fibers were used: 60 mm length with 0.8 mm diameter (aspect ratio of 75) and 30 mm length with 0.5 mm diameter (aspect ratio of 60). The steel fibers were galvanized and had a minimum tensile strength of 1100 MPa. The water–cement ratio was 0.38 and the percentage of fibers was 1.85% by weight of concrete and 0.57% by volume of concrete. A plasticizer was used in order to improve the workability of the mix. Concrete was compacted with a vibratory needle. The mixing procedure used in the manufacturing of concrete was as follows. The aggregates (blue granite with maximum dimension of 15 mm) and the sand were washed and dried before the process started. The constituents were introduced in the following order: water, cement, fibers, aggregates and sand. A small mixer with 200 dm<sup>3</sup> capacity was used.

The specimens remained in the molds for seven days covered by humid tissues after which they were cured at the natural environment of the laboratory (approximately 20°C temperature and 70% relative humidity).

---

\* Corresponding author. Tel.: +351-91-9397727.

E-mail addresses: pcachim@civil.ua.pt (P.B. Cachim), jafig@fe.up.pt (J.A. Figueiras), ppereira@ci.uminho.pt (P.A.A. Pereira).

Notation		$d\epsilon/dN, d\epsilon/dt$	secondary creep rate
$dE_f/dN, dE_f/dt$	fatigue modulus creep rate	$N$	fatigue life, number of cycles to failure
$d_{max}$	maximum displacement at failure in a fatigue test	$S$	stress level, fatigue strength
$d_{mon}$	envelope displacement (monotonic test) for a particular stress level	$S_{max}$	maximum stress level
		$S_{min}$	minimum stress level

Table 1  
Material characteristics and concrete composition

Materials	Composition (kg/m <sup>3</sup> )
Cement (Portland type II, class 32.5)	450
Sand (0–3 mm)	716
Aggregate (0–5 mm)	533
Aggregate (5–15 mm)	533
Water	171
Steel fibers (hooked-end)	
Series I: 30 mm length, 0.5 mm diam.	45
Series II: 60 mm length, 0.8 mm diam.	
Plasticizer (Rheobuild® 561)	4.5

The tested specimens were cylinders 150 mm in diameter and 300 mm in height. The top cylinder extremity was ground to ensure that both surfaces are parallel. Between the specimen and the load platens no interface material has been used.

Two series of compressive fatigue tests on plain concrete and fiber-reinforced concrete have been carried out. As it is intended to compare the performance of steel-fiber-reinforced concrete with that of plain concrete, batches of plain and fiber concrete were made in each series. In series I, 30 mm steel fibers were used. In this series, 17 specimens of plain concrete and 17 specimens of fiber concrete were cast. In each batch, five specimens were tested under monotonic conditions and the other 12 were tested under fatigue loading. In series II, 60 mm steel fibers were used. In this series, 36 specimens of plain concrete and 18 specimens of steel-fiber-reinforced concrete were cast. From these, six specimens were used to estimate the monotonic properties of the batch and the remaining specimens were tested under fatigue loading. Series I was tested within 30–60 days, while series II was tested within 18–20 months. This means that the maturity of the concrete of these two series is completely different. The reason for this difference in time was related with the setup of the fatigue testing procedure in the laboratory.

An MTS® (series 315) testing machine was used. The capacity of the system is 2700 kN with a maximum displacement of 100 mm. A digital controller allows that the tests can be carried out under displacement control

or load control (closed loop system). The complete process, including starting and terminating the test and acquiring and saving data, was computer controlled. The axial displacement of the cylinders was measured between the load platens by two LVDTs, thus avoiding any deformation of the testing machine to be included in the measured displacement.

The monotonic tests were carried out with displacement control with a speed of 10  $\mu\text{m/s}$ . The values of the force and the displacements were stored every 0.4 s. The fatigue tests were carried out with load control between two limits (with a sinusoidal force variation in time). The minimum stress level,  $S_{min}$ , is 10% of the monotonic strength and the maximum stress level,  $S_{max}$ , ranges from 60% to 90% of the monotonic strength. Before the cyclic process is started, the load is monotonically applied with displacement control (50  $\mu\text{m/s}$ ) until it reaches the maximum stress level. The frequency of loading used was 2.5 Hz. Data are acquired 10 times during each cycle and three different types of data acquisition have been used. First, the sampling rate of the initial 500 cycles is set to 25 Hz. After that, data of four cycles are acquired at a sampling rate of 25 Hz at intervals of 100, 500 or 2000 cycles depending on the load level. The results of the four cycles are then averaged to store a unique cycle. Finally, the last 300 cycles are recorded at a sampling rate of 25 Hz.

The test stopped after specimen failure or after half a million cycles in the case of series I and after a million cycles in the case of series II. This difference in the given number of cycles to stop the test was set because of restrictions in the use of the testing machine. The specimens that did not fail are named run-out specimens.

### 3. Results of the tests

#### 3.1. Monotonic test results

The results of the monotonic tests show that the compressive strength of concrete reinforced with 30 mm fibers was about 17% higher than the corresponding plain concrete strength. Contrasting with these results, it was observed that, in series II, the compressive strength

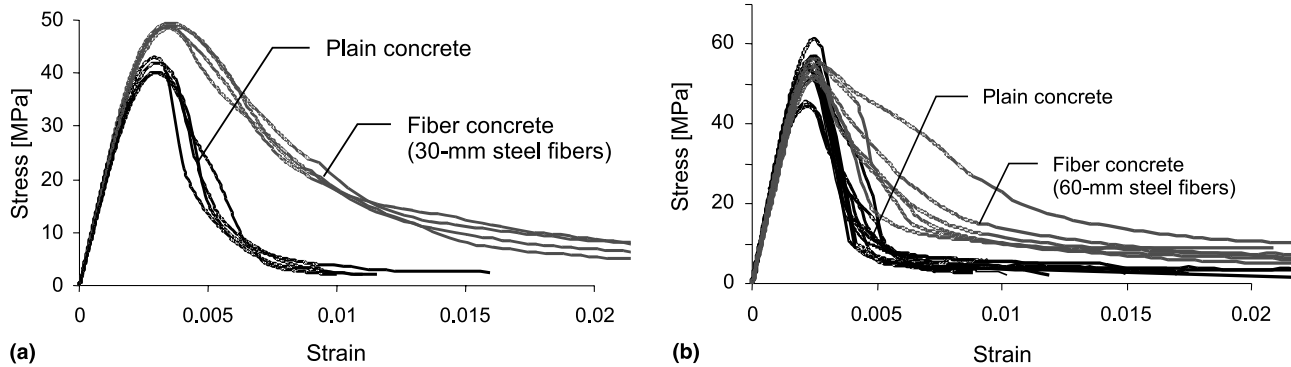


Fig. 1. Monotonic stress-strain diagrams for series I and II.

of concrete reinforced with the 60 mm fibers was identical to that of plain concrete. Nevertheless, no general conclusions can be deduced from these observations. With respect to the deformation of the specimen at the peak load and dissipated energy (defined as the area under the stress-strain diagram after peak load), it was observed that fibers increased both properties (see Fig. 1).

### 3.2. Stress level

Plotting the stress versus the number of cycles until failure (known as  $S-N$  diagrams or Wöhler diagrams) an assessment of the influence of the stress level on the fatigue life of concrete can be illustrated. However, when presenting the results of fatigue tests on an  $S-N$  basis, it must be kept in mind that the relative stress level ( $S$ ) is not known because the strength of that specimen is not known, which may explain by itself some scatter found on fatigue data. The fatigue life of concrete is represented in Fig. 2 for series I and in Fig. 3 for series II.

To represent the fatigue data, a power law between the stress level and the fatigue life is used. The regression equations and the regression coefficients for all test series are presented in Table 2. The regression equations

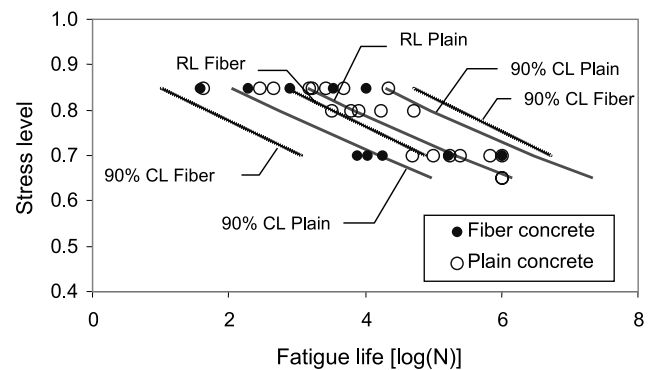


Fig. 3. Wöhler diagrams for series II.

(RL) and the 90% confidence limits (CL) are also plotted in these figures. From the observation of the Wöhler diagrams it is apparent that the scatter of data related to steel fiber-reinforced concrete is much greater than that of plain concrete. Additionally it was found that the fatigue data of concrete reinforced with 60 mm steel fibers show more scatter than concrete reinforced with 30 mm steel fibers.

The fatigue life of fiber-reinforced concrete was found to be smaller than that of plain concrete in series II while in series I the fatigue life of fiber concrete was slightly bigger than that of plain concrete. The shorter fatigue life of fiber-reinforced concrete in series II may be explained by several factors. The main reason is related to the fact that the fatigue phenomenon is related to initial imperfections, such as micro-cracks or voids, existing in concrete. Thus, the presence of fibers, especially bigger ones, may be an additional cause of imperfections, creating bridges between the aggregates and initial residual stresses. An effect of the size of the fibers relative to the size of the tested specimens could also possibly occur, since for the 60 mm fibers the ratio between the cylinder diameter and the fiber length is 2.5, which is a relatively low value. Another point arises from the fact that the used fibers are initially glued into bundles that should be separated during the concrete mixing. However, it was

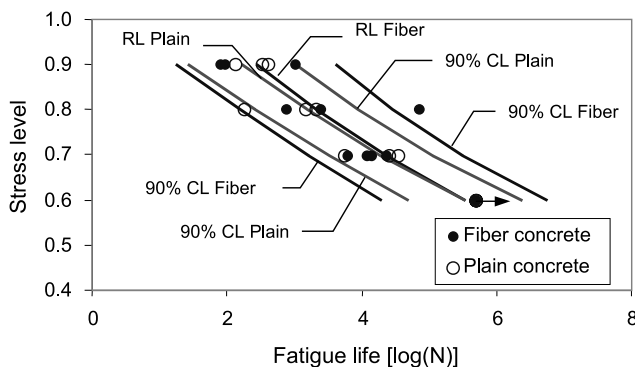


Fig. 2. Wöhler diagrams for series I.

Table 2

Regression equations for  $S$ – $N$  diagrams of plain and fiber concrete

Specimen series	Material	Regression equation	$r^2$
Series I: 30 mm fibers tested 1–2 months	Plain concrete	$\log(N) = 1.3528 - 25.7033 \log(S)$	0.924
	Fiber concrete	$\log(N) = 1.1529 - 24.1578 \log(S)$	0.781
Series II: 60 mm fibers tested 18–20 months	Plain concrete	$\log(N) = 1.3292 - 19.1663 \log(S)$	0.774
	Fiber concrete	$\log(N) = 1.6208 - 17.6600 \log(S)$	0.572

observed that some fibers remained glued creating a larger fiber, augmenting the bridge formation problem.

The smaller fatigue life found for series I, when compared with series II, may be explained by the age of concrete at the time of testing. The younger concrete, the 30 mm series, exhibits a more prominent nonlinear behavior on the ascending branch of the monotonic curve characterized by lower initial tangent modulus and higher peak strains. Since the non-linear behavior means damage at the internal structure then it is probable that for the same stress level the state of damage of series I was bigger than that of series II. Thus, it should be expected that the fatigue life of series I would be smaller than that of series II.

The effect of fibers on the compressive fatigue life of concrete is a subject that must be analyzed with some attention. In fact, Paskova and Meyer [12] testing fiber contents ranging from 0.25% to 1.0% found an increase of the fatigue life of fiber concrete augmenting with fiber content. However, for the steel fiber content of 0.75% the fatigue life was smaller than for all the other fiber contents, although bigger than that of plain concrete. The deviation of this result was attributed to difficulties in the production and compaction of the specimens. Additionally, in a previous work, Grzybowski and Meyer [6] stated that a reduction of the fatigue life of fiber concrete occurs for fiber contents above 0.25%. Yin and Hsu [17] reported the effects of steel fibers (fiber content of 1%) on the compressive fatigue life of concrete finding that the addition of fibers increases the fatigue life of concrete for stress levels above 0.70. However, these tests are somewhat different since the test specimens are plates ( $150 \times 150 \times 38 \text{ mm}^3$ ) sawed from blocks.

Therefore, the experimental results seem to confirm a dual effect of fiber reinforcement on the fatigue behavior of concrete. On one side, fibers bridge micro-cracks and tend to delay their growth, causing a strength increase. On the other side, fibers increase the initial micro-crack density causing a strength decrease. The combination of these opposing effects may cause an increase or a reduction of the fatigue life of fiber-reinforced concrete when compared with plain concrete. Special attention should then be taken during the mixing process to ensure that the fibers are very well dispersed in the concrete paste.

### 3.3. Deformations

The cyclic creep curves represent the evolution of the maximum deformation during a fatigue test plotted against the number of cycles. Three different stages can usually be observed in a cyclic creep curve: during the first 10–15% of the cycles, a rapid increase in deformation can be observed; then, an approximately linear branch, the secondary creep branch, can be observed up to about 85% of the fatigue life; finally, the deformation varies at an increasing speed until failure occurs. It is usually observed that a strong correlation exists between the slope of the secondary creep branch, the secondary creep rate,  $\dot{\epsilon}$ , and the number of cycles to failure [7,16]. This relation is linear when a logarithmic scale is used (Fig. 4). In Table 3 the regression equations for the secondary creep rate versus fatigue life are shown. It can be observed that an excellent correlation exists between these variables with the coefficients of correlation being higher than 0.99 for both types of concrete series. For series II it can be observed that for the same secondary creep rate the fatigue life of fiber-reinforced concrete was bigger. However, in series I, almost no differences are found between the two regression lines although a slightly increase of the fatigue life of fiber concrete was also observed for the same secondary creep rate. Additionally, it can be observed that, in all cases, the slope of the regression line is approximately the same. Similar findings have also been reported by other investigators (see [1,7,16]).

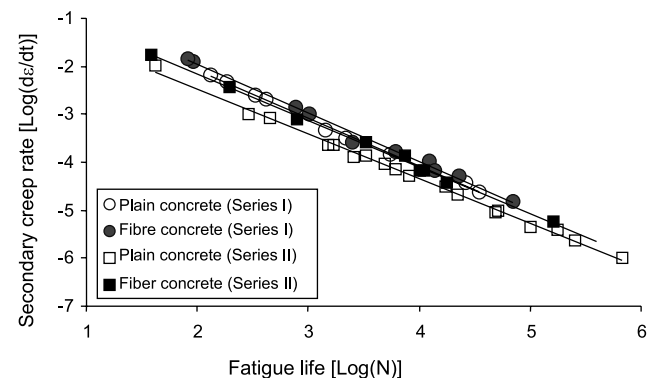


Fig. 4. Secondary creep rate versus fatigue life.

Table 3  
Regression equations for secondary creep rate versus fatigue life

Specimen series	Material	Regression equation	$r^2$
Series I: 30 mm fibers tested 1–2 months	Plain concrete	$\log(N) = -0.9975 \log(\dot{\epsilon}) - 0.0770$	0.997
	Fiber concrete	$\log(N) = -0.9850 \log(\dot{\epsilon}) + 0.076$	0.994
Series II: 60 mm fibers tested 18–20 months	Plain concrete	$\log(N) = -1.0725 \log(\dot{\epsilon}) - 0.6556$	0.996
	Fiber concrete	$\log(N) = -1.0298 \log(\dot{\epsilon}) - 0.2261$	0.996

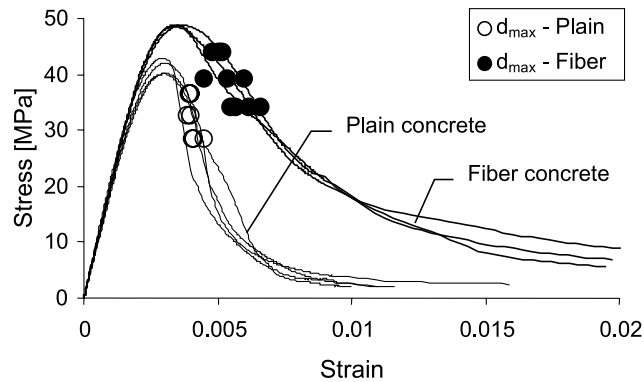


Fig. 5. Comparison of maximum deformation at failure with monotonic envelope (series I).

The fatigue life of fiber concrete is bigger than that of plain concrete for the same secondary creep rate. It can be understood with the help of Fig. 5, wherein the maximum deformation at failure,  $d_{\max}$ , is plotted over the monotonic stress–strain diagrams for the case of series I. The maximum deformation at failure is defined as the deformation corresponding to the maximum force of the last cycle supported by the cylinder. As expected, the final deformation at failure is larger for fiber concrete. Thus, if two specimens of both types of concrete fail for the same number of cycles, then the secondary creep rate must be greater for fiber concrete.

An important question regarding the fatigue behavior of concrete that is generally accepted in the literature is the existence of an envelope for deformations ([3,9] for plain concrete and [11] for fiber concrete). The envelope coincides with the monotonic loading curve or, at least, is very close to it. It is evident from the observation of Fig. 5 that the maximum deformations at failure agreed quite well with the monotonic envelopes. Although not presented in the figure, similar results were attained for series II. Hence, it can be concluded that the monotonic stress–deformation diagram can be used as an envelope for fatigue deformations.

### 3.4. Fatigue modulus

Fatigue modulus is defined as the ratio between the stress range and the corresponding deformation range

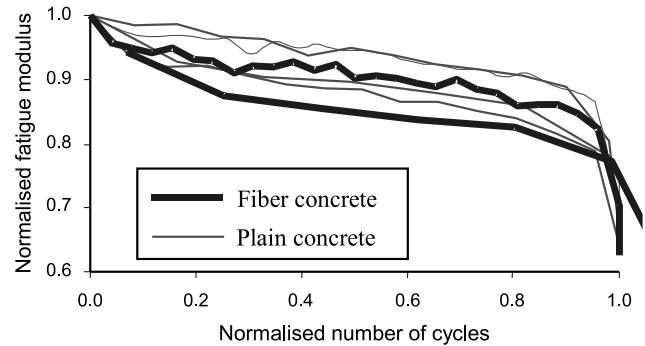


Fig. 6. Evolution of the fatigue modulus during fatigue tests for series I at  $S = 0.8$ .

within a load cycle. The effect of fatigue loading on the fatigue modulus can be observed in Fig. 6, where the number of cycles is normalized with the maximum number of cycles and the fatigue modulus is normalized with the initial fatigue modulus. Since the fatigue modulus is directly related with the deformations, because the stress range is constant, the same three different stages (see Fig. 6) can be observed during a fatigue test. The observed reduction of fatigue modulus is about 30% for all types of concrete.

### 3.5. Post-fatigue properties

A monotonic test has been carried out on the cylinders that do not fail after a predetermined number of cycles. The monotonic tests allow the assessment of the fatigue loading on the monotonic properties of concrete in order to establish the differences between the pre-fatigue and post-fatigue behavior. Facing the limited number of run-outs the presented results must be observed with caution.

Probably the run-out specimens were stronger than the other specimens tested at the same level, otherwise they would have failed. Consequently, it is expected that the strength of these specimens should be higher. It was observed that the monotonic strength of series I increases 16% in the case of plain concrete and 8% in the case of fiber-reinforced concrete. With respect to series II, average increases of 6% in the monotonic strength of plain concrete and of 15% in the case of fiber concrete

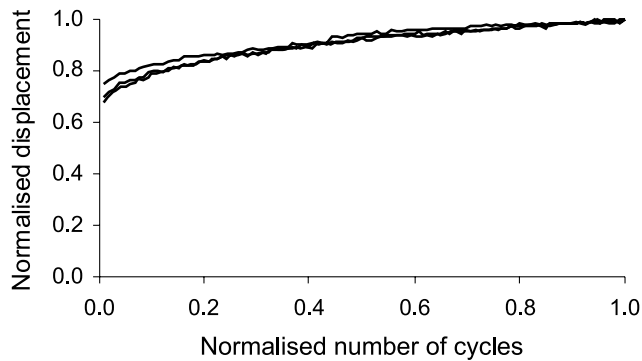


Fig. 7. Cyclic creep curve for fiber concrete run-out specimens (series II).

were found. These findings coincide with results presented in the previously mentioned RILEM and CEB reports [2,3,14], where increased strengths up to 15% of the monotonic strength are reported. In addition, Taliervo and Gobbi [16] found increases in strength up to 18% of the monotonic strength and Nelson et al. [10] found increases up to 39% of the monotonic strength.

The initial tangent modulus of series I increases 5 MPa for plain concrete and 8 MPa for fiber-reinforced concrete. In the case of series II, the initial tangent modulus increases 10% in the case of plain concrete and 16% in the case of fiber concrete. This is in agreement with the fact that higher strengths correspond to higher moduli. Nelson et al. [10] also found an increase in the tangent modulus (about 4%). The post-fatigue behavior also exhibits a linear stress–strain curve up to a higher percentage of the ultimate strength. An important aspect should be mentioned here in regard to the increase of the initial tangent modulus. The difference in the increase of the initial tangent modulus for series I and for series II was quite different. However, the specimens of series II exhibit a pre-fatigue initial tangent modulus about 35% higher than that of series I. Thus, it seems that the fatigue loading induced a similar beneficial effect to that of aging of concrete with respect to the initial tangent modulus.

The observed hardening effects may be explained by Fig. 7, where the cyclic creep curves of the run-out specimens of 60 mm fiber-reinforced concrete are plotted (similar results are attained for plain concrete and for series I). It can be seen that the rate of variation of the deformations is permanently decreasing. It seems that the specimen is not yet in a phase where damage prevails over the consolidation.

#### 4. Conclusions

The described experimental program pointed out some of the most relevant characteristics of the behavior

of plain and steel fiber concrete under compressive fatigue loading. An excellent agreement was found between the secondary creep rate and the number of cycles to failure. The existence of an envelope for deformations was also observed which means that the monotonic stress–strain curves might be used as a deformation failure criterion for concrete under fatigue loading. The fatigue modulus is also a very important property to accurately model individual load–unload cycles. The rate of variation of the fatigue modulus during a test is strongly correlated with the number of cycles to failure. An increase of some monotonic properties, initial modulus and strength, of the run-out specimens was observed.

The addition of fibers to concrete provides an increase in the deformation at failure. This additional ductility of fiber-reinforced concrete may be very important if stress redistribution between sections take place. The 60 mm fibers used in the experiments may be too long for the sectional characteristics of the specimens, creating conditions for a shorter fatigue life of fiber concrete.

The key to the success of improving the fatigue life of concrete with the addition of fibers seems to be related with the distribution of the fibers in concrete. In fact, if the fibers are not well dispersed in concrete, the addition of fibers may have a detrimental effect on the fatigue life of concrete.

#### References

- [1] Alliche A. Contribution a l'étude de l'endommagement du beton soumis a des sollicitations de fatigue. PhD Thesis, Ecole Central des Arts et Manufactures de Paris, 1988.
- [2] CEB. Fatigue of concrete structures – state of the art report. Bulletin d'Information no. 188, 1988.
- [3] CEB. Behaviour and analysis of reinforced concrete structures under alternate actions inducing inelastic response. Bulletin d'information no. 210, 1991.
- [4] Do M-T, Chao O, Aitcin P-C. Fatigue behavior of high-performance concrete. ASCE JM 1993;1:96–111.
- [5] Gao L, Hsu CTT. Fatigue of concrete under uniaxial compression cyclic loading. ACI Mater J 1998;Sept.–Oct.:575–81.
- [6] Grzybowski M, Meyer C. Damage accumulation in concrete with and without fiber reinforcement. ACI Mater J 1993;Nov.–Dec.:594–604.
- [7] Hordijk DA, Wolsink GM, Vries J. Fracture and fatigue behaviour of high strength limestone concrete as compared to gravel concrete. HERON 1995;40(2):125–46.
- [8] Hsu TC. Fatigue of plain concrete. ACI J 1981;78:292–305.
- [9] Karsan ID, Jirsa O. Behavior of concrete under compressive loadings. ASCE ST 1969;95:2543–63.
- [10] Nelson EL, Carrasquillo RL, Fowler DW. Behavior and failure of high-strength concrete subjected to biaxial-cyclic compression loading. ACI Mater J 1988;85(3):248–53.
- [11] Otter DE, Naaman AE. Properties of steel fiber reinforced concrete under cyclic loading. ACI Mater J 1988;July–Aug.:254–61.
- [12] Paskova T, Meyer C. Low-cycle fatigue of plain and fiber-reinforced concrete. ACI Mater J 1997;July–Aug.:273–85.

- [13] Ramakrishnan V, Meyer C, Naaman A, Zhao G, Fang L. Cyclic behavior, fatigue strength, endurance limit and models for fatigue behavior of FRC. In: Naaman A, Reinhardt, editors. High performance fiber reinforced cement composites. London: E & FN Spon; 1996.
- [14] RILEM. Long term random dynamic loading of concrete structures. *Mater Constr Paris* 1984;17(97):1–27.
- [15] Su ECM, Hsu TTC. Biaxial compression fatigue and discontinuity of concrete. *ACI Mater J* 1988;May–June:178–88.
- [16] Taliercio ALF, Gobbi E. Experimental investigation on the triaxial fatigue behavior of plain concrete. *Mag Concr Res* 1996;48(176):157–72.
- [17] Yin WS, Hsu TC. Fatigue behavior of steel fiber reinforced concrete in uniaxial and biaxial compression. *ACI Mater J* 1995;92(1):71–81.
- [18] Yin WS, Su E, Mansur M, Hsu TC. Biaxial tests of plain and fiber concrete. *ACI Mater J* 1988;86(3):236–43.